Analysis of Quality Factor of Damped Pendulums

Tian Ye
Henry Samueli School of Engineering and Applied Science, Univ. California Los Angeles

Chris Ong
College of Letters and Science, Univ. California Los Angeles

November 14, 2017

Abstract

In Classical Physics, a physical pendulum is a rigid body that is free to rotate around a single pivot. When the pendulum is displaced from its equilibrium position, it undergoes harmonic oscillation, given that the angle of displacement is small. Both amplitude and frequency of oscillation remain constant in an ideal simple harmonic oscillator. When a second force that is proportional to the velocity is acting on the body, it is known as a damped oscillation. This first portion lab aims to analyze the underdamped, overdamped, and critically damped motion of the pendulum. The second portion aims to compute and analyze the quality factor of a driven oscillation using various methods.

I. Introduction

This report discusses the resonance frequencies of a damped and undamped pendulum. The objective is to use the resonance frequency of a system to solve for the quality factor, or Q, of the system.

$$Q = \frac{1}{2}\tau\omega_r \tag{1}$$

$$Q \approx \frac{\omega_0}{\Delta\omega} \tag{2}$$

Where τ is the damping time, ω_r is the damped resonance frequency, ω_0 is the undamped resonance frequency, and $\Delta\omega$ is the full width of the resonance.[1]

II. Methods

The first portion of the experiment involves swinging an anchor-shaped wedge, both with and without damping effects from a pair of magnets. By setting the starting position of the pendulum so that it is within a single blade length of itself, we are able to apply small angle theorem. The tests were used to find the natural frequency of oscillation, f_0, and the necessary spacing of the damping magnets to achieve critical damping, respectively.
We next solved for the driving frequency of the system by placing the damping magnets at a spacing that would completely damp the oscillation within 5 to 10 seconds and recorded the damping time. We then drove the oscillation via a wave driver at various frequencies, recording the Lissajous figures at each frequency until it took upon the appearance of a circle, which occurs at the driving frequency of the system.

Using Equation 1, we then solve for Q using the data gathered from the various tests. We then plotted the frequencies of oscillation to solve for $\Delta\omega$. When the various frequencies are plotted together, a curve is created that peaks at the resonance frequency. The width of the curve when it is at $\frac{1}{\sqrt{2}}$ of its maximum height is $\Delta\omega$. Using this, we can then approximate Q using Equation 2.

III. Analysis

To solve for f_0, we plot the angular displacement versus time graph for underdamped,

overdamped, and critically damped oscillations.

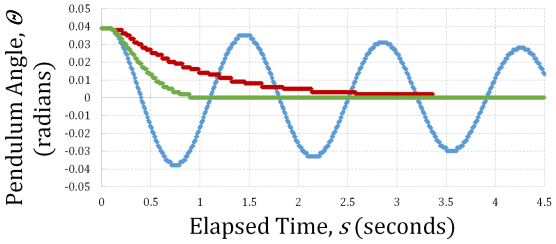

Figure 1: *Solving for f_0 and critical damping spacing.* The blue curve represents the amplitude vs time graph of an underdamped oscillation, the red curve an overdamped oscillation, and the green curve a critically damped oscillation. The spacing between the magnets in the three tests are (50 $\pm$ 1) mm, (10 $\pm$ 1) mm, and (16 $\pm$ 1) mm, respectively.

Viewing the Figure 1, we can then solve for f_0 by finding the elapsed time interval between each maxima of the underdamped oscillation and dividing that value by the number of elapsed maxima minus 1. We then take the inverse of the period to solve for frequency. To normalize the data, we repeat this process for multiple ranges of extrema and solve for the uncertainty of our calculated frequency by using Equation ii.13 from the Lab Manual:

$$\delta f = \frac{\sigma_f}{\sqrt{N}} \tag{3}$$

Where σ_f is the sample standard deviation and N is the number of data points.[1] Using the methods described above, we find f_0 to be (0.713 $\pm$ 0.005) Hz. Therefore, by multiplying f_0 by 2π, we find $\omega_0 = (4.48 \pm 0.03)$ Hz.
We then find a spacing between the magnets so that an undriven oscillation completely dies out between 5 and 10 seconds before testing our driven oscillations. After several tests, we choose a separation between the magnets of (30 $\pm$ 1) mm. We then repeat the steps performed above to find the frequency of oscillation of the damped pendulum.
From Figure 2 above, we calculate f of the damped oscillation to be (0.718 $\pm$ 0.004) Hz. By isolating the amplitude of the successive maxima of the function, we are then able to

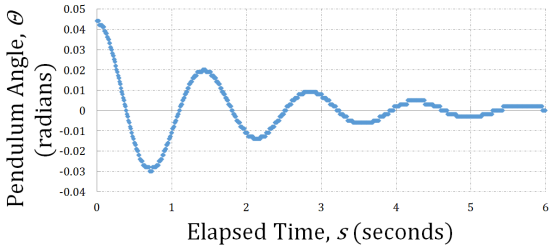

Figure 2: *Solving for f of damped oscillation.* The blue curve represents the amplitude vs time graph of the oscillation of the pendulum given the spacing between the damping magnets is (30 $\pm$ 1)mm.

calculate r, the ratio of successive maxima, to be 0.45 $\pm$ 0.01. Using this, we can then calculate the damping time, τ, using the following equation:

$$\tau = -\frac{T}{\ln\left[\frac{V(t+T)}{V(t)}\right]} \tag{4}$$

$$\tau = -\frac{T}{\ln[r]} \tag{5}$$

Where r is the ratio of successive maxima. We find τ = (1.74 $\pm$ 0.01) s. Note: the high uncertainty value is due to the compounded uncertainty of the maxima of the function and the period of the function - both of which are due to the limitations of the recording devices and their precision.
Then, via the usage of Lissajous figures, we determine the resonance frequency of the system.

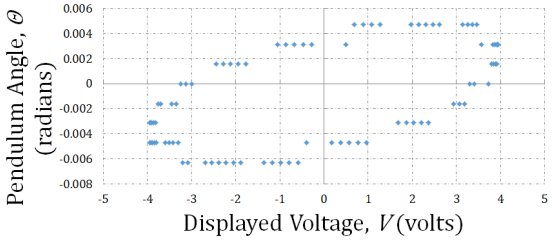

Figure 3: *Solving for resonance frequency of driven oscillation.* The blue Lissajous figure corresponds to a driving frequency of 0.63 Hz.

The ellipse of the Lissajous figure tilts depending on how far above or below resonance the current frequency is. Therefore, the Lissajous figure at resonance appears as a symmetrical

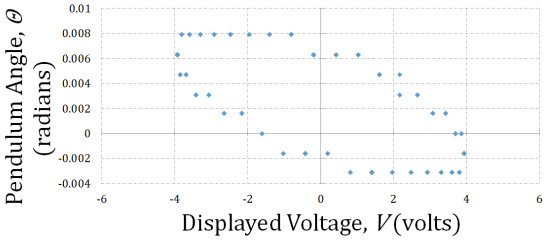

Figure 4: *Solving for resonance frequency of driven oscillation.* The blue Lissajous figure corresponds to a driving frequency of 0.75 Hz.

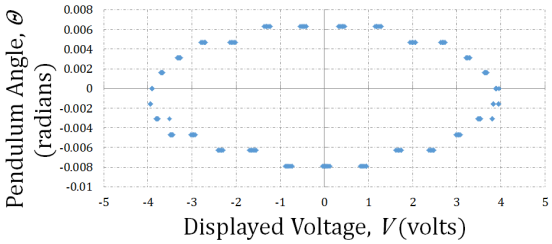

Figure 5: *Solving for resonance frequency of driven oscillation.* The blue Lissajous figure corresponds to a driving frequency of 0.69 Hz.

ellipse with no slant, which in this case is the figure corresponding to the driving frequency of (0.690 $\pm$ 0.001) Hz. Given that, we then know that $\omega_r = (4.335 \pm 0.006)$ Hz.
Referring back to Equation 1 and using the following equation, we find Q = (3.77 $\pm$ 0.01).

$$\delta Q = \frac{1}{2}\sqrt{(\tau\delta\omega_r)^2 + (\omega_r\delta\tau)^2} \qquad (6)$$

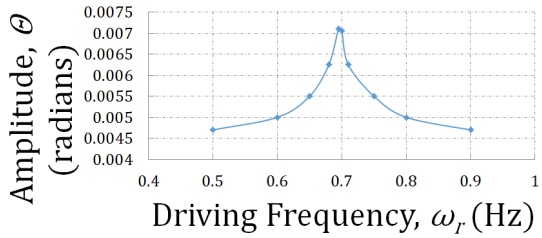

Figure 6: *Solving for $\Delta\omega$.* The curve is amplitude with respect to driving frequency.

We then use a second method to solve for the Q value via plotting the range of the amplitude frequencies. Using Figure 6, we can now approximate $\Delta\omega$, the width of the graph when the curve is at $\frac{1}{\sqrt{2}}$ of its maximum amplitude. In this case, $\Delta\omega = (1.26 \pm 0.12)$ Hz, following the conversion from frequency to angular frequency.
Referring back to Equation 2 and using the following equation, we find Q = (3.45 $\pm$ 0.16).

$$\delta Q = \frac{1}{2}\sqrt{\left(\frac{\omega_0}{\Delta\omega^2}\delta\Delta\omega)^2 + \left(\frac{1}{\Delta\omega}\delta\omega_0\right)^2\right)^2} \qquad (7)$$

Using a third method to solve for Q, we adjust the driving frequency until the amplitude of the pendulum is approximately $\frac{1}{\sqrt{2}}$ of the maximum amplitude.

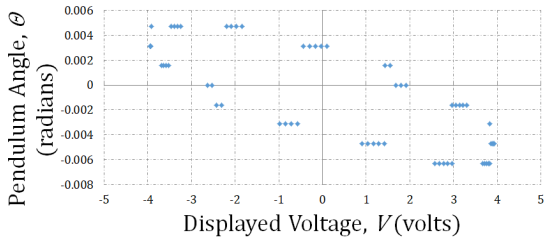

Figure 7: *Solving for $\Delta\omega$ of amplitude response curve.* The blue Lissajous figure corresponds to a driving frequency of 0.765 Hz.

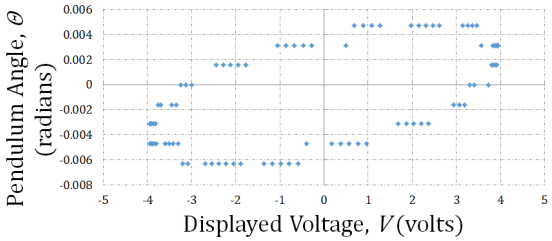

Figure 8: *Solving for $\Delta\omega$ of amplitude response curve.* The blue Lissajous figure corresponds to a driving frequency of 0.625 Hz.

The figures are both elliptical and tilt in opposite directions. Furthermore, if the midpoint between the two frequencies are taken, we find that the resonance frequency found using this method is 0.695 Hz, which is similar to the value calculated earlier. Using this, we find $\Delta\omega$ to be 0.88 Hz. Using Equation 6.15 from the Lab Manual, we find a third Q value of (4.92 $\pm$ 0.3).

IV. Discussion

When we compare the two Q values that were obtained from Equation 1 and Equation 2, we find that there is a nontrivial discrepancy between the values. The value derived from Equation 1 however is likely to be more accurate than the value derived from Equation 2, as the Q value derived from Equation 2 is heavily dependent on estimation of $\Delta\omega$. Due to that fact the uncertainty of $\Delta\omega$ has a large effect on the uncertainty of the Q value derived from Equation 2. When comparing the uncertainties as a percentage of the Q value for the Q values obtained from both Equation 1 and Equation 2, we find that the percentages are 0.2% and 4.6%, respectively.

While the Q value obtained from the third method is most different from the other two, it is more likely more accurate than the others, primarily due to the fact that it does not require guessing at the resonance frequency via visual analysis of Lissajous figures as is the limiting factor in the first method, and does not require guessing at a value of $\Delta\omega$ visually, as the second method requires. Furthermore, it is not constrained to only values of Q that are significantly greater than 1, as is in the case of Equation 2.

Viewing the values of the quality factors themselves, we note that they are both relatively low. This implies that the oscillations are of a similar order magnitude and that they both quickly damped to 0, both of which are true for the case of this experiment.

A primary source of systematic uncertainty in this experiment is the potential difference in recording times of the wave driver and rotation sensor for the Lissajous figures. The analysis on the current figures is operated under the assumption that both the data points for the voltage from the wave driver and the angle measured from the rotation sensor are being recorded at the same instance of time. However, if one is earlier than the other, it will in turn skew the tilt of the Lissajous figure and consequently skew the estimated resonance frequency of the pendulum.

A second source of systematic uncertainty is friction between the pivot of the pendulum and the pendulum itself, which in turn creates its own damping force that is a function of the amplitude of oscillation. This would in turn indicate that as the pendulum approaches steady state, the force of damping from friction increases as well, which in turn skews the resonance frequency and consequently the Q value obtained from Equation 1.

References

[1] Campbell, W. C. *et al*. Physics 4AL: Mechanics Lab Manual (ver. August 31, 2017). (Univ. California Los Angeles, Los Angeles, California).

Analysis of Standing Waves on a String

Tian Ye
Henry Samueli School of Engineering and Applied Science, Univ. California Los Angeles

Chris Ong
College of Letters and Science, Univ. California Los Angeles

November 28, 2017

Abstract

Harmonic motion is exhibited by nonrigid systems such as a string, in which each particle undergoes vertical displacement as waves travel through the medium. While the particles themselves have no transverse motion, they are able to carry energy from one point to another in the form of a transverse wave. When both ends of the string are fixed as nodes, the apparent transverse motion of the oncoming waves cancel out with the reflecting waves and results in zero apparent transverse motion. This in turn creates waves that appear to not move but rather oscillate in place, known as standing waves. The frequency at which no nodes appear between the two ends of string and at which the amplitude of oscillation is maximized is known as the fundamental frequency. Integer multiples of the fundamental frequency create additional nodes between the two ends of the string. The objective of this lab is via the analysis of a transverse wave on a string to find the fundamental frequency of a string. Additional objectives include observing modes of standing wave oscillations and to observe the effects of an added boundary condition in the middle of the string.

I. Introduction

This report discusses the fundamental frequency of a string with two fixed ends, and the associated harmonic frequencies that accompany it. The objective is to use the transverse velocity of a single wave on the string to serve as the starting point to solve for the fundamental frequency. It then uses the calculated value for the fundamental frequency to explore the higher harmonics associated with it.

II. Methods

The first portion of the experiment involves stretching a string over a wave driver, looping it over a pulley, and hanging masses on the far end to put tension on the string. A photodiode near the pulley end of the string records the light intensity produced by a laser beam spot on the string.

The linear mass density of the string was calculated measuring the mass and length of the unstretched string. The linear mass density of the stretched string was than calculated based on the length of the stretched (unclamped) string and its mass.

We next use the wave driver to send pulses down the string and the photodiode to record the light intensity. The photodiode is set up so that the light intensity correlates with the vertical displacement of the string. By measuring the time intervals between the maximum amplitudes, we were then able to calculate the velocity of the traveling wave.

We next use the wave driver to send sinusoidal pulses down the string and via the usage of Lissajous figures calculate the resonance frequency of oscillation. We then multiply the resonance frequency, f_r, by n to find the nth harmonics.

The final part of the experiment involved creating a node in the center of the string via a clamp and observing its effects on the amplitude of oscillation of the standing wave at various harmonics.

III. Analysis

Using the following equation, we first solve for the wave speed using the following equations:

$$v = \sqrt{\frac{T}{\mu}} \tag{1}$$

$$\delta v = \sqrt{\left(\frac{1}{2\sqrt{T\mu}}\delta T\right)^2 + \left(\frac{1}{2}\sqrt{T}\mu^{-\frac{3}{2}}\delta\mu\right)^2} \tag{2}$$

Where T is the tension of the string and μ is the linear mass density.
However, we must also take into account that the linear mass density of the string, μ, changes as the string stretches from the weight of the masses. Therefore, the equation for the linear mass density of the stretched portion of the string is:

$$\mu = \frac{m - L_{\text{clamped}}(\mu_0)}{L_{\text{unclamped}}} \tag{3}$$

Where L is the respective lengths of the string, m is the total mass of the string, and μ_0 is the unstretched linear mass density of the string.

Table 1: String Data for Various Masses

$m = [(1.50 \pm 0.05) \times 10^{-2}]$ kg $\mu_0 = [(6.62 \pm 0.08) \times 10^{-3}]$ kg/m $L_{\text{clamped}} = [(1.5 \pm 0.1) \times 10^{-2}]$ m		
Tension (N)	Unclamped Length (m)	μ (kg/m)
3.92 ± 0.01	2.282	$(6.5 \pm 0.6) \times 10^{-3}$
4.41 ± 0.01	2.329	$(6.4 \pm 0.7) \times 10^{-3}$
4.90 ± 0.01	2.397	$(6.2 \pm 0.7) \times 10^{-3}$

The uncertainties of the linear mass density are found using the following equation:

$$\delta\mu = \sqrt{\left(\frac{L_c}{L_u}\delta\mu_0\right)^2 + \left(\frac{1}{L_u}\delta m\right)^2 + \left(\frac{m - L_c(\mu_0)}{{L_u}^2}\delta L_u\right)^2} \tag{4}$$

Where L_c and L_u refer to the clamped and unclamped lengths of the string, respectively.
Using the values in Table 1, the transverse wave speed along the string can now be predicted via the use of Equations 3 and 4. The values are compared with the experimental values further below in Table 2.
To find the experimental values of the transverse wave speed, we use a wave driver to send signals down the string. The photodiode then picks up the fluctuations in light intensity caused by change of y-component displacement of the string. The fluctuations are displayed in the following figure:

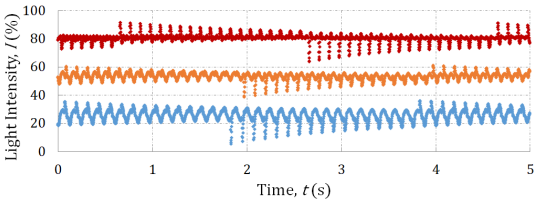

Figure 1: *Solving for v for various masses.* The blue points represent the amplitude vs time graph of the string with tension of (3.92 ± 0.01) N, the orange points represent a string with tension of (4.41 ± 0.01) N, and the red points represent a string with tension of (4.90 ± 0.01) N. Each curve is normalized about a different point so that they are easier to view.

We then find the time interval between each peak, t, and divide double the distance between the wave driver and pulley, L, by the time interval to solve for v:

Table 2: Experimental Wave Speeds

$L = (3.060 \pm 0.002)$ m		
Tension (N)	Time Interval (s)	Velocity (m/s)
3.92 ± 0.01	0.122 ± 0.001	25.08 ± 0.04
4.41 ± 0.01	0.114 ± 0.001	26.84 ± 0.03
4.90 ± 0.01	0.106 ± 0.001	28.87 ± 0.03

The uncertainty of the experimental velocity is found using the following equation:

$$\delta v = \sqrt{\left(\frac{1}{t}\delta d\right)^2 + \left(\frac{d}{t^2}\delta t\right)^2} \tag{5}$$

The following table compares the predicted values of velocity with the experimental ones:

Table 3: Wave Speed Comparison

Tension (N)	Predicted (m/s)	Experimental (m/s)
3.92 ± 0.01	24.6 ± 1.1	25.08 ± 0.04
4.41 ± 0.01	26.3 ± 0.9	26.84 ± 0.03
4.90 ± 0.01	28.1 ± 1.0	28.87 ± 0.03

The next part of the lab involved attempting to find the fundamental mode of a standing wave with the two fixed ends of the string being the

clamp and the pulley. We begin by testing driving frequencies around a predicted resonance frequency using the following equation:

$$f = \frac{nv}{2L} \tag{6}$$

Where n refers to the harmonic number, v is the velocity of a transverse wave on the string, and L is the length of the string. Plugging in our experimental values into the above equation, we estimate the frequency for the fundamental mode of the string to be around 9.43 Hz.

We then try several frequencies in the ballpark of the estimated frequency to find the frequency of the fundamental mode. By observing which frequency produces the largest amplitude, we are then able to find the frequency associated with the fundamental mode. We find that a driving frequency of (9.540 $\pm$ 0.003) Hz produces the largest amplitude of standing waves.

Via the usage of Lissajous figures, we then verify the accuracy of the experimental resonance frequency. While the Lissajous figures are not in the form of ellipses, we are still able to "measure" a form of symmetry by viewing how much the figure shifts over time. We define a symmetric figure as one that traces approximately the same path with each iteration.

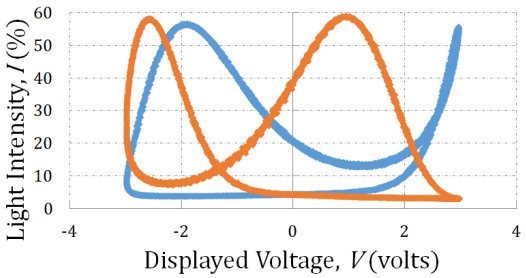

Figure 2: *Verification of harmonic frequencies.* The orange points and blue points represent Lissajous figures corresponding to driving frequencies of 19.08 Hz and 28.62 Hz, respectively. These represent the $n = 2$ and $n = 3$ modes, respectively.

We use this method of verification as we find the harmonics for increasing n values (refer back to Equation 8). Furthermore, we note that $n - 1$ nodes appear between the two end nodes of the string as we increase harmonics.

Using the above verification methods, we find the $n = 2, 3, 4$, and 5 frequencies to be equal to 19.08 Hz, 28.62 Hz, 38.16 Hz, and 47.70 Hz, respectively. We note that as the harmonic modes increase, the amplitude of oscillation decreases.

Next, we pinch the string at the midpoint, therefore artificially creating a node at the point. We find that for the even values of n, there is little effect to the amplitude of oscillation of the string, as there is already naturally a node at that point. However, for odd n values such as $n = 5$, we find that the amplitude of oscillation almost disappears entirely. This is due to the fact that by preventing oscillation at that point, we are effectively enforcing a new boundary condition onto the string. Therefore, the conditions that were used to calculate the fundamental mode no longer apply.

We also note that we were only able to visually identify nodes and anti-nodes to approximately the 9th mode. At that point, the amplitude of oscillation becomes negligible to the point at which visually there are no longer any nodes or antinodes.

Finally, we attempt to create a node at the point where the photodiode is located over the string. The laser is approximately 50 mm from the pulley, and therefore, the end of the string. We also know that each mode creates 2^{n-1} equally spaced nodes between the two nodes that make up the end of the string. From this, we can use math to predict which mode would create a node any point.

If we take the total length of the string, 1580 mm, and divide it by 50 mm to partition it into m equally spaced 50 mm portions, we find that we divide it into 32 portions. 32 is equal to 2^5, and using that knowledge, we can therefore predict that the 6th mode will create a node 50 mm from the end of the string. When we input a driving frequency of 57.24 Hz, we see that a node is indeed created at that point.

IV. Discussion

When we compare the experimental and the predicted values of the transverse waves on the string, we see that there is a notable difference between the values. However, they nonetheless

fall within the uncertainties of each other, and despite the large uncertainties, none of them exceed 5% of the value.

When we view the experiment as a whole, we can note that there are many sources of systematic uncertainty within it. The effects of a possible source of systematic uncertainty can be seen within the calculations for the fundamental frequency: regardless of whether the experimental or predicted transverse velocity was used in Equation 6, we find that the calculated fundamental frequency of the string to be lower than the experimental one. This can be associated with the photodiode and laser system.

A second source of systematic uncertainty can be found during the section during which we clamp down the center of the string. As the clamp we use does not clamp a single point at the node, but rather instead has a definite width, it affects the amplitude of the even numbered harmonics as well - albeit not to the same extent as it does odd numbered harmonics.

Finally, a third problem that became more prevalent as the driving frequency of the string increased was the horizontal motion of the string: as the string oscillated vertically, it also experienced horizontal motion that increased with driving frequency. This in turn affects the accuracy of the photodiode measurements, as the change in light intensity cannot be attributed to vertical motion alone.

References

[1] Campbell, W. C. *et al*. Physics 4AL: Mechanics Lab Manual (ver. August 31, 2017). (Univ. California Los Angeles, Los Angeles, California).